

Supporting Information

Edin et al. 10.1073/pnas.0901894106

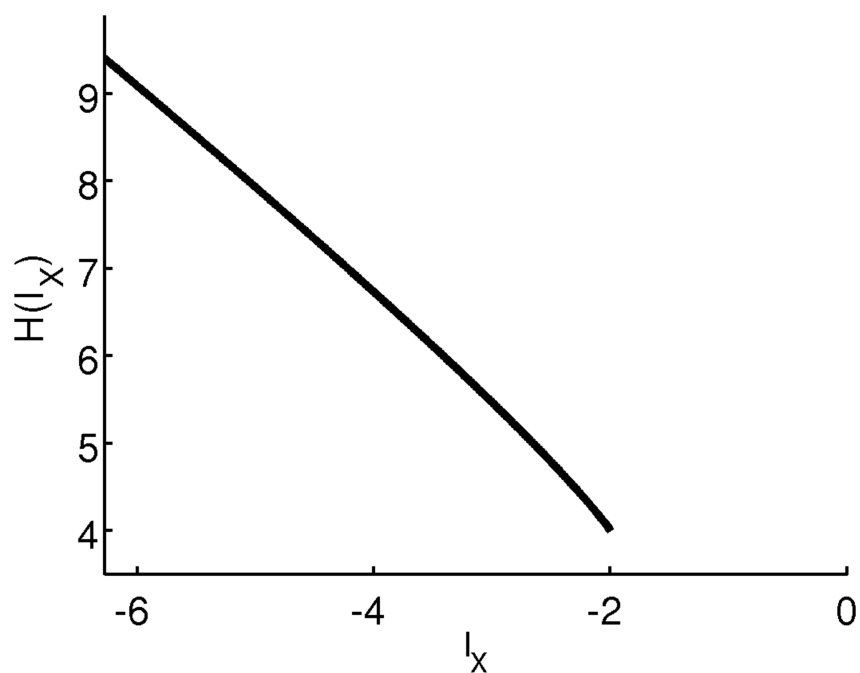


Fig. S1. Graphical representation of $H(l_x)$ in the equation for p_{cap} (Eq. 2) with $f(l) = (1 + e^{-l})^{-1}$

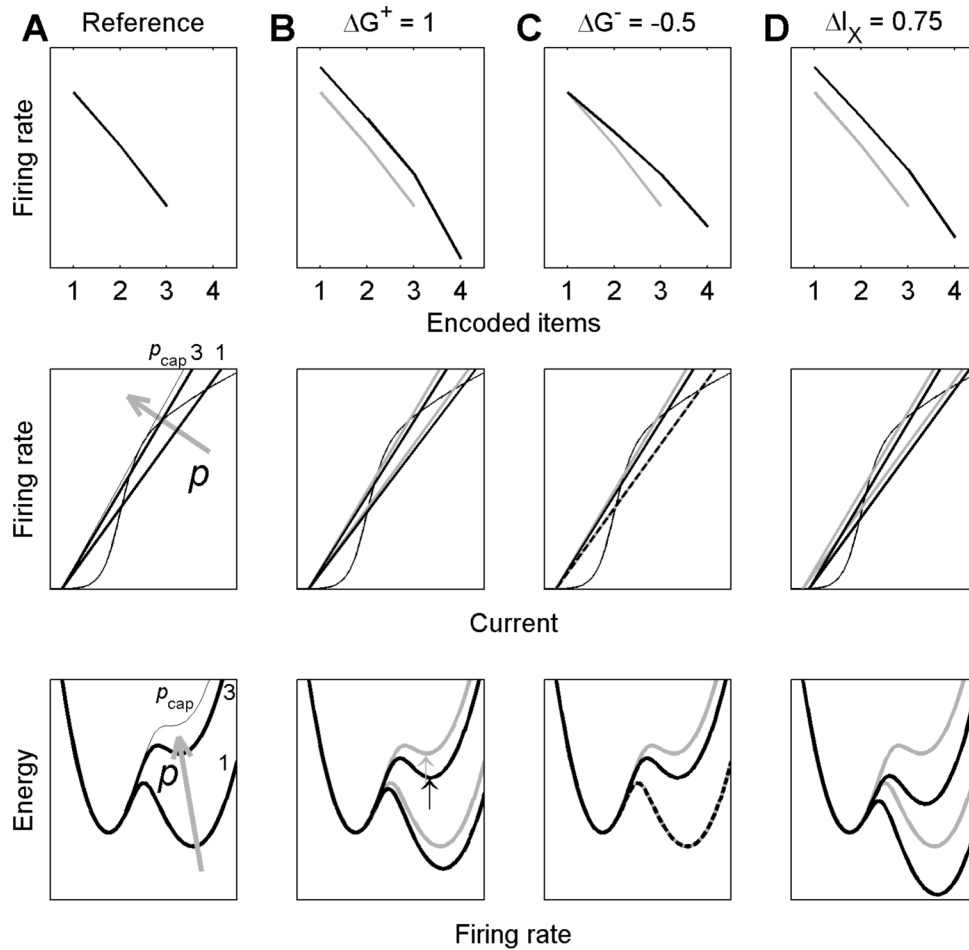


Fig. S2. Effect of changes in G^+ , G^- , or I_X on memory capacity and persistent activity. Changes in parameters that lead to improved capacity generally increase network activity. (*Top*) Firing rate of memories at different loads. (*Middle*) Graphical solutions of the capacity equation for two different loads, $p = 1$ and 3. As p increases, the line representing the effective network synaptic strength shifts leftward. (*Bottom*) Potential energy landscape of the network at loads 1 and 3. Energy minima represent stable states. (A) Reference parameter set used in Fig. 2: $A = 0.1$, $G^+ = 22$, $G^- = 2$, $I_X = -6.25$. When load equals capacity (thin line; here, $p_{cap} = 3.57$) the synaptic line is tangential to the neuronal-input output curve in the *Middle*. (*Bottom*) The energy minimum corresponding to the memory state disappears at capacity (thin line). (B) Increasing capacity from 3 to 4 by increasing G^+ leads to increased persistent activity at the same load (arrows indicate memory activity at load $p = 3$). For comparison, the reference network is shown in gray. (C) Same for G^- . (D) Same for I_X . Generally, networks that have higher capacity caused by a change in a G^+ , G^- , or I_X also have higher activity at the same load.

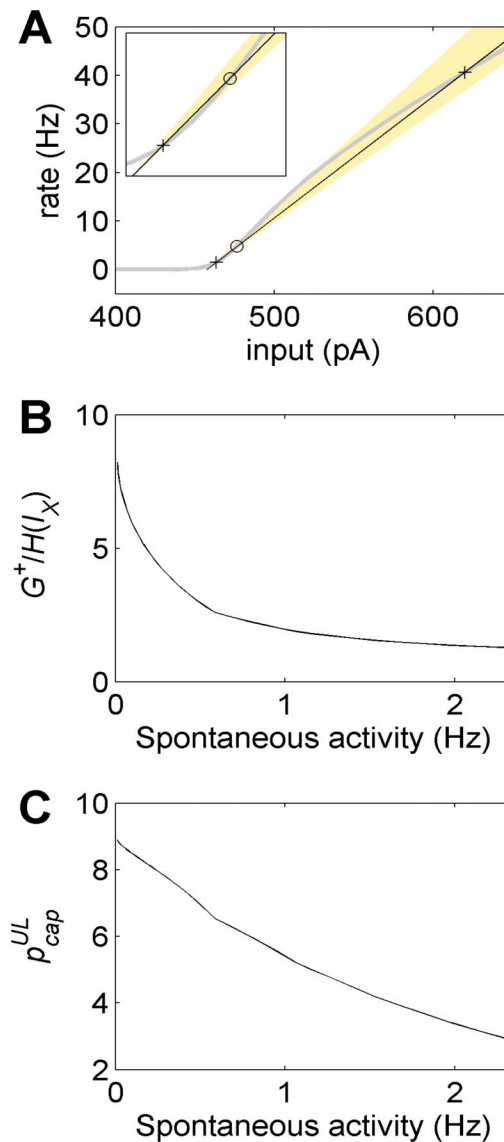


Fig. S3. Working memory capacity in a balanced network. (A) The network is stable when the line and the curve intersect in three places. For the value of I_X in the figure, the golden area represents the region of stable memory activity. The size of this area is determined by the ratio between G^+ and $H(I_X)$, which determines the right and left border of the area. (B) $G^+/H(I_X)$ is in turn determined by the spontaneous activity. For spontaneous rates above ≈ 1.5 , $G^+/H(I_X) < 1.5$. (C) Having determined $G^+/H(I_X)$, Eqs. 3 and S6 (see *SI Appendix*) can now be used to calculate p_{cap}^{UL} for a given level of spontaneous activity. Note that although p_{cap}^{UL} in Eqs. 3 and S6 (see *SI Appendix*) is a continuous variable, only a discrete number of stimuli can be presented, making capacity an integer number. The following parameters were used. Standard deviation of input current, determining the linearity of the $f-I$ curve: $\sigma = 0.001$. $w: 0.1$.

Table S1. Maxima in the conjunction analysis of fMRI activation in either M3–C3 or M5–C5 contrasts; group analysis

Location		Area*	BA [†]	MNI coordinates	t statistic	Cluster size
Superior parietal lobule	R		7	16, -74, 52	6.69	12,494 ^I
	L		7	-14, -70, 52	4.93	12,494 ^I
Middle occipital gyrus	L		17/18	-34, -88, 14	5.08	12,494 ^I
	R	e	17/18	36, -90, 14	5.12	12,494 ^I
Superior frontal gyrus (SFG)/	R	b	6	30, -4, 56	4.02	1,852 ^{II}
Middle frontal gyrus	L		6	-24, -2, 58	3.24	372
Medial frontal gyrus (mSFG)	R	d	8/32	8, 18, 50	2.16	1,852 ^{II}
Inferior frontal gyrus (IFG)	R	c	47	34, 20, 6	3.41	443
	L		47	-30, 22, -4	2.92	199
Middle frontal gyrus (dlPFC)	R	a	9/46	52, 34, 32	2.94	791 ^{III}
	R	a	46	42, 44, 22	3.56	791 ^{III}
	R	a	10/46	38, 54, 26	2.12	791 ^{III}
	L		46	-46, 48, 14	3.01	144 ^{IV}
	L		10/46	-32, 62, 8	1.94	144 ^{IV}

Clusters identified testing the global null hypothesis of no activation in either M5–C5 or M3–C3 contrasts, with a threshold at $P = 0.05$ after correcting for multiple comparisons using the false-discovery rate procedure. Only clusters larger than 100 voxels are shown.

*Identification of areas tagged with lower-case letters in the brain illustration of Fig. 4B.

[†]Brodmann area (BA) estimation from Talairach Daemon Client v2.0 (<http://ric.uthscsa.edu/resources>) and xjView (<http://people.hnl.bcm.tmc.edu/cuixu/xjView/>). I, II, III, and IV indicate same activation cluster.

Table S2. Cell parameters

Parameter	E cells	I cells
N	1,024	256
C_m	0.5 nF	0.2 nF
g_L	25 nS	20 nS
E_L	-70 mV	-70 mV
V_{res}	-60 mV	-60 mV
V_{th}	-50 mV	-50 mV
τ_{ref}	2 ms	1 ms
r_x	1,800 Hz	1,800 Hz

N , number of cells; C_m , membrane capacitance; g_L , leak conductance; E_L , leak reversal potential; V_{res} , reset potential; V_{th} , spike threshold potential; τ_{ref} , refractory period time constant; r_x , rate of external afferents. For an explanation of these parameters and the equations they govern, see Compte A, Brunel N, Goldman-Rakic PS, Wang XJ (2000) Synaptic mechanisms and network dynamics underlying spatial working memory in a cortical network model. *Cereb Cortex* 10:910–923.

Table S3. Synaptic parameters

Parameter	AMPA	NMDA	GABA
τ_s	2 ms	100 ms	10 ms
α_s		0.5 ms^{-1}	
τ_x		2 ms	
V_{rev}	0 mV	0 mV	-70 mV

τ_s , decay time constant for s , the fraction of open channels; α_s , saturation constant; τ_x , rise time constant; V_{rev} , reversal potential. For an explanation of these parameters and the equations they govern, see Compte A, Brunel N, Goldman-Rakic PS, Wang XJ (2000) Synaptic mechanisms and network dynamics underlying spatial working memory in a cortical network model. *Cereb Cortex* 10:910–923.

Table S4. Connectivity

Parameter	IPS	dIPFC
Connection strength G , nS		
E→E, AMPA	0.0	0.0
E→E, NMDA	0.684	0.968
E→I, AMPA	0.0	0.0
E→I, NMDA	0.479	0.723
I→E*	3.643	3.660
I→I	2.896	2.832
X→E†	→Table S5	3.000
X→I	5.800	2.3803
Connection curve width σ , degrees		
E→E	9.4	
E→I	32.4	
I→E	32.4	
Connection curve height J^+ , unitless		
E→E	5.7	
E→I	1.4	
I→E	1.4	

For an explanation of the parameters and the equations they govern, see Compte A, Brunel N, Goldman-Rakic PS, Wang XJ (2000) Synaptic mechanisms and network dynamics underlying spatial working memory in a cortical network model. *Cereb Cortex* 10:910–923.

*Connections from I cells are always GABA_AR-mediated.

†X, external afferents.

Table S5. Parameters varied in simulations

Figure	$G_{X \rightarrow E}$, nS	dIPFC \rightarrow IPS, nS	dIPFC rate, Hz
1B	6.6		
1 C and D	6.4, 6.45, 6.5		
1E	6.55–6.725		
3 B and C	6.525	9	
3D	6.525	0–15	
3E	6.525	6.525	0–95
3F	6.625–6.775		

For an explanation of these parameters and the equations they govern, see Compte A, Brunel N, Goldman-Rakic PS, Wang XJ (2000) Synaptic mechanisms and network dynamics underlying spatial working memory in a cortical network model. *Cereb Cortex* 10:910–923.

Other Supporting Information Files

[SI Appendix](#)